Nanoscale

MINIREVIEW

View Article Online
View Journal | View Issue

Cite this: *Nanoscale*, 2024, **16**, 14707

Advances in biomimetic AIE nanoparticles for diagnosis and phototherapy

Joe H. C. Chau,[a] Michelle M. S. Lee,[a] Eric Y. Yu,[a] Ryan T. K. Kwok,[a] Jacky W. Y. Lam,*[a] Jianwei Sun[a] and Ben Zhong Tang*[a,b]

Received 31st March 2024,
Accepted 11th July 2024

DOI: 10.1039/d4nr01417k

rsc.li/nanoscale

This minireview provides an overview of the recent advancements in the development of biomimetic Aggregation-Induced Emission (AIE) nanoparticles and their applications in disease diagnosis, phototherapy, and photoimmunotherapy. AIE nanoparticles can be engineered to enable efficient image-guided photodynamic and photothermal therapies, however, challenges related to immune defense and target specificity persist. To overcome these, coating biomimetic materials on the surface of AIE nanoparticles, which mimic the features and functions of native cells, have emerged as a promising solution. This minireview will highlight the synthesis strategies and discuss the biomedical application of biomimetic AIE nanoparticles.

1 Introduction

In recent years, there has been a remarkable surge in the development of advanced nanomaterials for biomedical applications. Specifically, the field of nanomedicine has witnessed significant progress in the areas of diagnosis and phototherapy,[1,2] thanks to the maturation of optical technologies. The applications of nanomaterials in elucidating biological and physiological activities, as well as conducting therapeutic trials, have garnered considerable attention. In particular, biomimetic strategies involving the use of biomaterials to endow native biological activities and features hold great promise in designing effective nanomaterials. The wide range of biomaterials available for coating nanoparticles to endow biomimetic properties include cell membranes sourced from blood cells, cancer cells, and extracellular vesicles.[3,4] The use of extracted cell membranes as bioactive coating endows nanoparticles with similar biological activity as the parent cells including targeting ability as well as potential surface ligands. Cell membrane camouflaged biomimetic nanoparticles retain some important physiological functions and activities such as cell communication and signal transduction. Such design rationales can afford the nanoparticle core with intrinsic advantages of enhanced cellular interaction, targeting specificity, prolonged blood circulation, better biocompatibility, and reduced toxicity.[3] In addition to cell membrane coatings, other biomimetic strategies involve incorporating proteins as nanoparticle cores and attaching biomolecules on nanoparticle surfaces such as antibodies, aptamers, and targeting peptides.[5] Among the choice of fluorescent materials, organic fluorogens offer a more tailored and less toxic alternative for biomedical applications as inorganic nanomaterials have concerns about potential toxicity.[6,7] Nonetheless, many organic fluorogens exhibit aggregation-caused quenching (ACQ) effects when formulated into organic nanoparticles, leading to reduced imaging quality and therapeutic efficacy. Although biomimetic strategies may enhance uptake and cellular interactions, the main functionality derived from the fluorescent nanomaterial is still hindered by the detrimental ACQ effect.

Fortunately, fluorogens with aggregation-induced emission (AIE) property (AIEgens) can avoid the shortcomings of ACQ after being encapsulated into nanoparticles,[8,9] thus improving the imaging quality and treatment efficiency. AIEgens exhibit high emission efficiency and photosensitivity in their aggregated state, making them suitable for the fabrication of water-dispersible nanoparticles with maintained fluorescence and photostability. Moreover, these AIEgens can be integrated with emerging techniques, including photodynamic therapy (PDT), photothermal therapy (PTT), and photoacoustic imaging, to enable in-depth *in vivo* bioimaging and image-guided surgery.[10–17] The field of cancer therapy, in particular, has seen significant advancements with the integration of AIE nanoparticles.[18–20] Conventional treatment options such as surgery, chemotherapy, and radiation therapy often face limitations in their efficacy and associated side effects.[21] PDT and

[a]*Department of Chemistry, Hong Kong Branch of Chinese National Engineering Research Center for Tissue Restoration and Reconstruction, Division of Life Science, State Key Laboratory of Molecular Neuroscience, and Department of Chemical and Biological Engineering, The Hong Kong University of Science and Technology, Clear Water Bay, Kowloon, Hong Kong, 999077, China.*
E-mail: tangbenz@cuhk.edu.cn, chjacky@ust.hk
[b]*School of Science and Engineering, Shenzhen Institute of Aggregate Science and Technology, The Chinese University of Hong Kong (CUHK-Shenzhen), Shenzhen, Guangdong 518172, China*

PTT have emerged as promising noninvasive approaches to improve cancer treatment. PDT involves the use of photosensitizers to generate reactive oxygen species (ROS), which selectively damage cancer cells while also activating immune cells. On the other hand, PTT utilizes photothermal agents that convert light energy into heat, leading to localized damage in cancer cells. By combining AIE-active photosensitizers or photothermal agents with chemotherapy, radiotherapy, or immunotherapy, the overall cancer therapy effect can be improved.

Despite the advantages of AIEgens in image-guided surgery, it still faces challenges related to immune defense and lack of specificity to the target site. With that consideration, the combination of biomimetic strategies with AIEgens presents a win–win situation that not only overcomes the drawbacks of the ACQ effect but also improves the efficacy of AIEgens by endowing intrinsic biological activity. Biomimetic AIE nanoparticles are AIE-active nanoparticles coated with biomaterials that mimic the features and functions of native cells or use biomaterials as the nanoparticles core with AIE material attached to the surfaces. Such nanoparticles inherit the high emission efficiency and photosensitivity of AIEgens while benefiting from the enhanced targeting capabilities, prolonged circulation times, and immune system evasion provided by

Table 1 Summary of biomimetic AIE nanoparticles for disease diagnosis and phototherapy

Biomimetic strategies	Inner cores	Outer layers	Application	Ref.
AIEgen-binding biomolecular NP	Bacteriophage	AIEgen (TVP-T)	PDT for intracellular bacterial infection	33
	BSA	AIEgen (TPAQ-Py-PF_6)	PDT for colon cancer	23
	BSA	AIEgen (BITT)	Photo-chemotherapy for bladder cancer	24
	Glucan	AIEgen (HBTTPEP)	Monitoring of transplant immune response	25
	Yeast NP	AIEgen (QMC12)	Photodynamic–immunotherapy for melanoma	26
Ligand-binding AIE NP	AIE NP (BPBBT)	Anti-CXCL9 peptide	Diagnosis of myocarditis	35
	AIE NP (*t*-BuPITBT-TPE)	Cell-penetrating peptide (Tat)	Tracing the repair and treatment of spinal cord injury	36
Cell membrane encapsulated AIE NP	AIE NP (P2-PPh_3)	Erythrocyte membrane	Photodynamic–immunotherapy for melanoma	37
	AIE NP (PF3-PPh_3)	Erythrocyte membrane	PDT for carcinoma	40
	AIE NP (TPE-BT-DPTQ)	Macrophage membrane	Photothermal lysis of virus	43
	AIE NP (BBT-C6T-DPA (OMe))	Neutrophil membrane	Antibacterial PTT	44
	AIE NP (TPE-BT-BBTD)	Macrophage membrane	PTT for tuberculosis	48
	AIE NP (DCPy)	Platelet membrane	PDT for orthotopic colon cancer	39
	AIE NP (TBP-2)	Platelet membrane	PDT for cancer stem cells	45
	AIE NP (TBP-2)	Platelet membrane	PDT for breast cancer	46
	AIE NP (PF3-PPh_3)	Platelet membrane	Photodynamic–immunotherapy for carcinoma	47
	AIE NP (MeTIND-4)	Dendritic cell membrane	Photodynamic–immunotherapy for carcinoma	38
	AIE NP (Fs)	Dendritic cell membrane	Photodynamic–immunotherapy for carcinoma	41
	AIE NP (BPBBT)	Dendritic cell membrane	PTT for carcinoma	42
	AIE NP (PTI)	MCF-7 cell membrane	PDT for breast cancer	49
	AIE NP (TTPA)	B16-F10 cell membrane	Photodynamic–immunotherapy for melanoma	50
	AIE NP (Pep-TPE)	Transferrin receptor aptamer-modified brain metastatic tumor cell membrane	Gene-induced therapy for brain tumor	51
	AIE NP (DHTDP)	4T1 cell membrane	PTT for carcinoma	52
	AIE NP (P-TN-Dox)	4T1 cell membrane	Chemo-photothermal synergistic therapy for carcinoma	53
	AIE NP (TPS-2)	4T1 cell membrane	PDT for carcinoma	54
	AIE NP (DCCP)	Lewis lung carcinoma cell membrane	PDT for lung cancer	55
	AIE NP (TT3-*o*CB)	Tumor cell-derived exosome	PTT for carcinoma	56
	AIE NP (MBPN-TCyP)	Dendritic cell-derived small extracellular vesicle	Photodynamic–immunotherapy for carcinoma	57
	AIE NP (BITT)	Lung cancer cell-derived exosome	Photo-mediated immunotherapy for lung cancer	58
	AIE NP (*o*BBT-DPNA)	Macrophage-derived exosomes	Near-infrared tumor imaging	59
	AIE NP (TPE-BBT)	Tumor cell-derived exosome	PTT for breast cancer	60
	AIE NP (DPDPy)	Platelet-derived exosome	Photodynamic–immunotherapy for breast cancer	61

Ref. – reference number, NP – nanoparticle, PDT – photodynamic therapy, PTT – photothermal therapy.

biomimetic coatings. This synergy results in more precise and efficient image-guided phototherapy, improved therapeutic efficacy, and broader applicability.

In this review, we aim to provide an overview of the recent advancements in biomimetic AIE nanoparticles for diagnosis and phototherapy. We will highlight the synthesis strategies and discuss the application of biomimetic AIE nanoparticles (Table 1). By summarizing these advancements, we hope to inspire the precise design of biomimetic AIE nanomaterials with optimized functions and structures for a range of biomedical applications.

2 Synthetic strategies of biomimetic AIE nanoparticles

2.1 AIEgen-binding biomolecular nanoparticles

Biomimetic nanoparticles offer a promising approach for incorporating AIEgen's functionality without extensive modification. By simply binding AIEgens onto biomolecule-based nanoparticles, phototherapy capabilities can be imparted. This attachment typically relies on hydrophobic interaction and hydrogen bonding, organic AIEgens can insert into the hydrophobic domain of biomolecules such as bacterium-like particles,[22] bovine serum albumin (BSA),[23,24] and glucan.[25,26]

Proteins play crucial roles in various cellular processes and possess exceptional structural integrity and functional diversity, making them ideal candidates for modification and reprogramming.[27,28] Among them, serum albumin, the most abundant protein in the blood, has been extensively studied for nanoparticle fabrication due to its versatility and biocompatibility.[29] Tang and Feng groups reported the successful insertion of cationic TPAQ-Py-PF_6 into the hydrophobic pocket of BSA, resulting in BSA nanoparticles with improved colloidal stability and biocompatibility.[23] Importantly, the immobilization of TPAQ-Py-PF_6 within BSA restricts intramolecular motions, favoring the generation of the excited triplet state in aggregates. Furthermore, the rich electron microenvironment of BSA provides the necessary substrates for $OH^{\bullet}$ radical generation.

Glucan particles (GPs), derived from yeast, hold promise as targeting agents for macrophages by mimicking yeast's behavior during intestinal infections.[30–32] GPs were prepared by treating yeast with sodium hydroxide and hydrochloric acid, followed by extraction with isopropyl alcohol and acetone. AIEgens bind with β-glucan and form aggregate within GPs and, as reported by Xie, Tang, Zhang, and Jin groups (Fig. 1A).[25] In a recent development, Tang, He, and coworkers reported AIE-armored bacteriophage-DNA nanoconjugates for efficient elimination of intracellular bacterial infection (Fig. 1B).[33] The preparation of bacteriophage nano-bioconjugates involved the amino-carboxyl reaction between DNA and MS2 phage, followed by the binding of positively charged AIEgens (TVP-T) to the DNA *via* electrostatic interactions. Taking advantage of the surface anchoring provided by DNA, the resulting bioconjugates resemble spherical nucleic acids and exhibit the ability to enter macrophages and target intracellular bacteria under the guidance of the bacteriophage.

2.2 Ligand-binding AIE nanoparticles

Alternatively, AIE nanoparticles can also serve as cores, with ligands attached to their surfaces as part of a biomimetic approach. These AIE nanoparticles, synthesized using the nanoprecipitation method and employing maleimide derivative DSPE-PEG_{2000}-Mal as the encapsulation matrix, allow for the conjugation of proteins and peptides with sulfhydryl groups to the maleimide groups on the nanoparticle surface.[34]

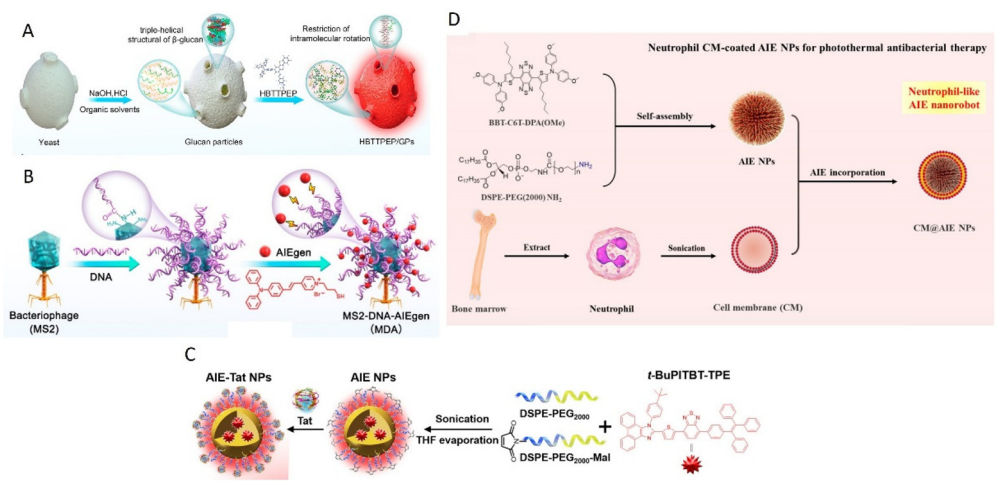

Fig. 1 Different synthetic strategies of biomimetic AIE nanoparticles. (A) Preparation process of biomimetic AIE-active glucan particles (HBTTPEP/GPs). Reproduced with permission from ref. 25. Copyright 2021 American Chemical Society. (B) Preparation of bacteriophage nanobioconjugate. Reproduced with permission from ref. 33. Copyright 2024 American Chemical Society. (C) Preparation of cysteine-modified trans-activator of HIV-1 transcription bound AIE nanoparticles (AIE-Tat NPs). Reproduced with permission from ref. 36. Copyright 2022 Wiley. (D) Synthesis of neutrophil-like AIE nanorobot (CM@AIE NPs). Reproduced with permission from ref. 44. Copyright 2023 American Chemical Society.

Song, Wang and Zhang groups demonstrated the conjugation of an anti-CXCL9 polypeptide with end-group modified sulfhydryl on NIR-II AIE nanoprobes for the early diagnosis of myocarditis.[35] In the acute phase of myocarditis, the inflammatory chemokine of CXC ligand 9 (CXCL9) positive macrophages are abundantly produced. The anti-CXCL9 sequence peptides are tailor-synthesized to specifically target CXCL9-expressing macrophages.

Besides, Rong *et al.* utilized a cysteine-modified trans-activator of transcription of HIV-1 (Tat) as a cell-penetrating peptide, enabling NIR AIE nanoparticles (AIE-Tat NPs) attached with Tat to monitor stem cell transplantation therapy for spinal cord injury (Fig. 1C).[36] AIE-Tat NPs could label umbilical cord mesenchymal stem cells to achieve long-term visual tracking over 28 days of transplanted cells *in vivo* with no significant interference of cell activity.

2.3 Cell membrane encapsulated AIE nanoparticles

Cell membrane camouflaged nanoparticles have emerged as effective drug delivery carriers, offering improved targeting efficiency and drug retention. Generally, three types of cells are exploited for delivery of AIEgens through cell membrane-based carriers: blood cells,[37–48] cancer cells,[49–55] and exosome vesicles.[56–61]

Upon injection into the bloodstream, nanoparticles initially encounter the immune system defenses, with phagocytes attempting to clear the nanoparticles through phagocytosis.[62,63] This leads to a shorter circulation time for the nanoparticles and reduced therapeutic efficacy. To prolong circulation time and shield the nanoparticles from immune cells, utilizing native blood cells as the membrane coating for nanoparticles proves to be a solution. Various blood cell types, such as erythrocytes,[37,40] macrophages,[43,44,48] platelets[39,45–47] and dendritic cells,[38,41,42] have been used to coat AIE nanoparticles. AIE nanoparticles are prepared by nanoprecipitation to form the cores, followed by coating the blood cell membranes onto the cores through coextrusion. Tang, Li, and Zhang groups reported the development of neutrophil-like biomimetic AIE nanoparticles for precise PTT and inflammation alleviation (Fig. 1D).[44] AIE nanoparticles were synthesized *via* nanoprecipitation using DSPE-PEG_{2000} as the doping matrix. The isolated neutrophil cell membrane from BALB/c mouse bone marrow was then used to coat the AIE nanoparticles. The camouflage with blood cell membranes enables the encapsulated AIE nanoparticles to evade immune system clearance and reach targeted sites such as tumors and bacteria.

Utilizing cancer cell membranes allows for the exploitation of their homologous cancer targeting capabilities and extended blood circulation half-life. Tang, Zhang, Hou, and Wang groups synthesized Trojan horse-like nano-AIE aggregates for anticancer photodynamic therapy.[49] They encapsulated AIEgens inside PLGA nanoparticle cores and coated them with MCF-7 cell membranes. Homologous MCF-7 cells exhibited the highest uptake of nanoparticles compared to other cancer cell lines (HeLa, 4T1, and T24) and displayed the strongest fluorescence signal. Thus, the cancer cell membrane coating facilitates the navigation of AIE nanoparticles toward corresponding cancer regions, enabling effective phototherapy. In addition to cancer cell membranes, exosome membranes also offer improved cancer targeting capabilities. Exosomes are extracellular vesicles secreted by all cell types carrying nucleic acids, proteins, lipids, and metabolites.[64] Exosomes are mainly involved in intercellular communication and exosome membranes can express CD47 providing immune evasion ability.[65] Macrophage-derived exosomes exhibit increased binding to integrin αvβ3, enabling exosome-encapsulated nanoparticles to possess specific tumor targeting abilities.[66] Sun, Chen, and their colleagues reported the encapsulation of hydrophobic AIEgens into tumor-associated macrophage-derived exosomes using a simple nanoprecipitation method.[59] Exosomes derived from tumor cells or macrophages are isolated through ultracentrifugation first, then applied as an encapsulation matrix during nanoprecipitation or through extrusion with AIE nanoparticles.

3 Biomedical applications of biomimetic AIE nanoparticles

3.1 Disease diagnosis

Fluorescence bioprobes with AIE characteristics are ideal tools for early disease diagnosis owing to their high sensitivity, selectivity, and brightness in bioimaging. However, fluorescence probes are less competent mainly due to poor bio-target specificity. In comparison, the integration of biomimetic nanotechnology can greatly improve the targeting specificity to achieve early diagnosis and disease study. Song, Wang, and Zhang groups reported the use of CXCL9+ macrophage-targeted NIR-II AIE nanoprobes for the early diagnosis of myocarditis.[35] In this work, a highly emissive NIR-II AIEgen, namely BPBBT, was used as the fluorescent probe to achieve a deep tissue penetration depth and high-quality intravital imaging property. To increase the targeting specificity of this AIE probe to the inflammatory site of myocarditis, BPBBT was then encapsulated by the amphiphilic matrices of DSPE-PEG and DSPE-PEG-MAL, followed by the surface modification of anti-CXCL9 peptides to obtain CXCL9+ macrophages-target nanoprobes. The surface modification of the anti-CXCL9 peptide of the biomimetic AIE nanoparticles takes full advantage of the specific ligand–receptor interaction with CXCL9+ macrophages given their abundance and dominance during the acute phase of myocarditis. Experimental findings demonstrated that the biomimetic AIE nanoparticles are capable of being phagocytosed by macrophages to a greater extent than the nanoparticles without modification due to CXCL9 binding. This work has further demonstrated *in vivo* imaging diagnosis of myocarditis using EAM mice as models. Results depicted that the EAM mice group injected with biomimetic AIE nanoparticles gave a clear signal with a visible heart outline, which indicates that the nanoparticles could contribute to the diagnosis of acute phase myocarditis.

Fluorescence tumor imaging is a popular research area due to its potential for tumor diagnosis from the blurred bound-

aries between normal tissue, but it has challenges of lacking precise tumor targeting property of traditional fluorescence probes. One of the examples is the diagnostic efficacy of glioblastoma multiforme, which is severely hampered by the existence of blood brain barrier that restricts most diagnostic agents from approaching the tumor sites. Wu, Liu, Xia and coworkers reported the use of transferrin receptor (TfR) aptamer to enhance blood brain barrier penetration of biomimetic nanocomplexes for intracellular transglutaminase 2 (TG2) imaging in glioma (Fig. 2).[51] This strategy involves the loading of AIE-active Pep-TPE to hollow MnO_2 nanoparticle core, followed by its encapsulation into TfR aptamer-modified brain metastatic B16-F10 cell membrane to form biomimetic nanocomplexes. The nanoparticles camouflaged by brain metastatic melanoma-derived B16-F10 enhance blood brain barrier penetration based on its brain metastatic nature and interaction between brain metastatic tumor cell surface receptor and endothelial cell adhesions. In addition, surface modification of TfR aptamer further enhances blood brain barrier crossing through specific ligand binding with the brain-metastatic tumor cell-surface receptor to help the nanocomplex reach glioma cells. The combination of receptor-mediated transcytosis and brain metastatic cell membrane camouflage provides a dual capability for penetration of blood brain barrier. The overexpression of TG2 in glioblastoma multiforme triggers Pep-TPE aggregation and fluorescence turn on for tumor diagnosis. The specific tumor targeting ability with a high signal-to-noise ratio of the designed biomimetic nanocomplex was revealed by *in vitro* and *in vivo* results. Sun and Chen and coworkers reported another strategy for NIR-II AIEgens encapsulated within nanometer-sized exosomes for tumor imaging.[59]

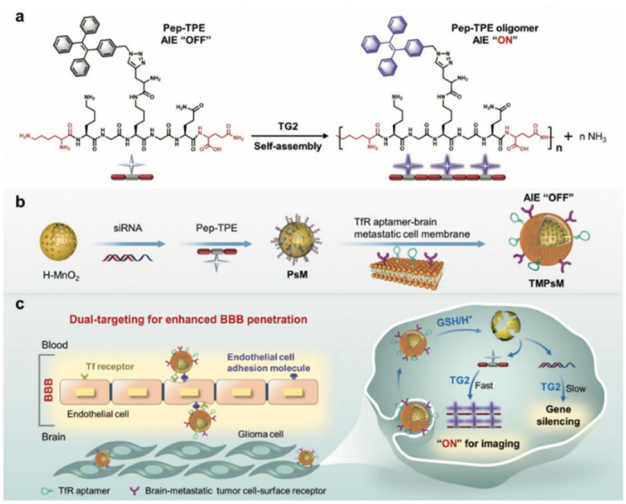

Fig. 2 Schematic illustration of the preparation and working mechanism of biomimetic nanocomplexes for glioblastoma multiforme diagnosis. (a) The AIE fluorescence turn on property of Pep-TPE with the presence of endogenous TG2. (b) The preparation process of TMPsM. (c) Schematic diagram of the dual-targeting TMPsM across the blood–brain barrier to brain tumors for simultaneous *in situ* self-assembly imaging and RNAi therapy of glioma. Reproduced with permission from ref. 51. Copyright 2022 Wiley.

NIR II AIE fluorescent nanoparticles were encapsulated by tumor associated macrophage-derived exosomes, which can enhance the homology with M2-phenotype tumor associated macrophage overexpressed in tumor cells, thereby ensuring the tumor targeting property. The further *in vivo* studies of the presented AIE biomimetic nanoparticles demonstrated the excellent tumor accumulation ability, which is capable of being applied for efficient imaging and diagnosis of specific tumors.

3.2 Phototherapy

Phototherapy holds extensive potential in disease treatment by employing light to trigger therapeutic effects. Common phototherapies such as PDT and PTT harness light to generate cytotoxic ROS and heat to damage the targeted site.[64] Despite their potential, limitations such as low targeting and biocompatibility exist in using photosensitizers or photothermal agents. In comparison, biomimetic nanotechnology stands out by virtue of its targeting capabilities and biosafety. Through a unique biological interface, modification with cell membranes, proteins, lipids, and DNA can facilitate immune response, targeted delivery and uptake, and better biodistribution, ultimately improving therapeutic performance. Tang's group reported biomimetic aggregates for homologous targeting of cancer by coating photosensitizers with active cancer cell membranes.[49] AIEgen (PTI) aggregates were first encapsulated into PLGA and further coated by MCF-7 cell membrane by electrostatic adsorption to form MCFCNPs. The homologous targeting strategy of MCFCNPs revealed the faster and highest uptake by MCF-7 cancer cells as evidenced by the stronger fluorescence intensity than PTI aggregates. The bionic function and homologous targeting of MCF-7 cells were confirmed by the amount of adhesion molecules on the surface of MCFNPs and their similarity with the MCF-7 cells. This is believed to be the prerequisite for homologous targeting with MCF-7 cells but no other cancer cell types. In addition, the biocompatibility of MCFCNPs confirmed negligible cytotoxicity. Interestingly, MCFCNPs showed improved ROS generation efficiency with doubled fluorescence enhancement of H2DCFH-DA compared to PTI aggregates. The *in vivo* PDT efficiency study demonstrated that the half-maximal inhibitory concentration of MCFCNPs and PTI aggregates against MCF-7 cells viability was 1.9×10^{-6} M and 3×10^{-6} M respectively, reflecting that the cell membrane coating strategy improved the PDT therapeutic efficiency. In addition, Tang's group utilized the homologous cell membrane loading strategy to enhance tumor-targeting PTT performance. Similarly, DHTDP aggregates were first encapsulated into DSPE-PEG. DHTDP nanoparticles were further camouflaged by 4T1 cancer cell membrane to give DHTDP NP@M.[52] As expected, DHTDP NP@M showed a stronger *in vitro* PTT effect and complete *in vivo* tumor ablation than DHTDP NP owing to the promoted cellular uptake efficiency and homologous targeting capability.

Besides cancer treatment, biomimetic strategy can amplify the effectiveness of phototherapy for bacterial infection treatment by enhancing precision and accuracy. Liao and col-

leagues developed a biomimetic nanoparticle for combined therapy of drug-resistant bacterial infections.[67] A laser-activatable AIE-Tei@AB NVs nanobomb was prepared by encapsulating AIE-PEG_{1000} nanoparticles, teicoplanin antibiotic, and ammonium bicarbonate into lipid nanovesicles.

The design rationale for lipid nanovesicle biomimicry is to reduce the binding of teicoplanin to plasma proteins, thereby ensuring adequate delivery of the antibiotic to the infected site. This lipid nanovesicle delivery system enhances the focal targeting of teicoplanin, increasing its effectiveness against infections. Without the lipid nanovesicle encapsulation, teicoplanin would bind to the plasma protein resulting in insufficient delivery to the infected sites. Upon laser activation, the AIE components undergo both photodynamic and photothermal actions, and the ammonium bicarbonate is thermally decomposed to generate gas bubbles, which disintegrate the lipid nanovesicles, allowing the simultaneous release of teicoplanin. The synergistic PDT, PTT, and pharmacological therapy maximize bactericidal efficiency at the infected site. AIE-Tei@AB NVs strategy showed complete inhibition of multidrug resistant (MDR) *S. aureus*, MDR *E. coli*, and MDR *P. aeruginosa*, confirming its broad-spectrum bactericidal effect. *In vivo* study further confirmed that MRSA-induced abscess mice treated with AIE-Tei@AB NVs and laser activation showed much higher bacterial clearance and improved wound healing rates. Given the complex antigenic composition of *Mycobacterium*, targeting of *M. tuberculosis* remains challenging. Recently, Liao's group developed pre-activated macrophage membrane-coated nanoparticles for PTT of tuberculosis (Fig. 3).[48] Macrophages stimulated by *M. marinum* expressing specific surface receptors were used for nanoparticle coating to achieve targeting of granulomas and *M. tuberculosis*. Transcriptomic analysis and characterization revealed activation of pattern recognition receptors and upregulation of toll-like receptors on macrophage cell membrane surface upon *M. marinum* stimulation. The toll-like receptors can recognize distinct pathogen-associated molecular patterns and their expression dramatically increased with increasing time of *M. marinum* stimulation. *In vitro* study demonstrated BBTD@M NPs exhibited specific targeting capability to *M. marinum* and H37Ra bacilli and subsequent PTT treatment showed complete eradication of bacteria with extensive disintegration and breakage. It is worth mentioning that BBTD@M NPs only showed specific targeting capability to *M. marinum* and H37Ra bacilli and no other bacterial species, confirming the feasibility of biomimetic macrophage stimulation with specific pathogens. *In vivo* studies showed that BBTD@M NPs accumulate in the granulomas of the lung, and subsequent PTT induced a stronger bactericidal effect than antibiotics. Biomimetic engineering integrates the advantage of natural cells and nanomaterials, creating a synergy that allows for the development of highly efficient therapeutic agents.

3.3 Photoimmunotherapy

Cancer immunotherapy has achieved impressive success in the field of tumor treatment, due to its use of the patient's own immune system to remove tumor cells. However, this strategy demonstrates only 40% tumor response, as well as drastically lower overall clinical response in solid tumor therapy. Meanwhile, the intense metabolism of cancer cells leads to hypoxia and a lack of crucial nutrients in the tumor micro-environment, which hinders the function of immune cells.

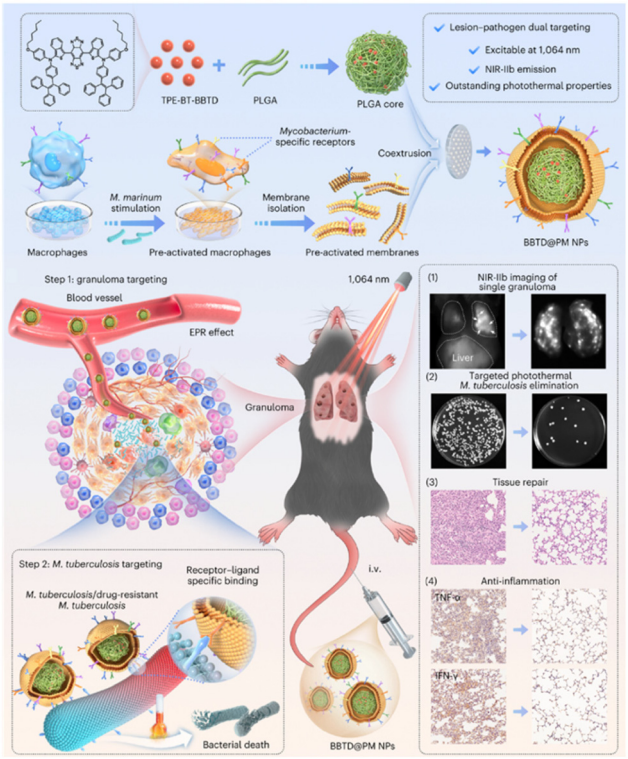

Fig. 3 Schematic diagram of the preparation of BBTD@PM NPs and mediated lesion–pathogen dual targeting and NIR-IIb imaging-guided photothermal therapy for tuberculosis. Reproduced with permission from ref. 48. Copyright 2024 Springer Nature.

Tang, Wang, Liu and coworkers reported biomimetic nanoplatform loaded with AIE photosensitizer and glutamine antagonist (CTTPA-G) to regulate nutrient partitioning for antitumor immunotherapy (Fig. 4).[50] The biomimetic nanoplatform, composed of a B16-F10 cancer cell membrane (CC-M), is engineered to achieve specific delivery of AIE photosensitizers and glutamine antagonists. CTTPA-G inherits the expression proteins of CC-M, allowing for precise targeting and visualization of B16-F10 cells. The biomimetic design enables prolonged *in vivo* circulation and homologous targeting, facilitating improved accumulation at tumor sites. The loaded glutamine antagonist can satisfy the glucose and glutamine required by T cells, which inhibit tumor glutamine metabolism, reverse the hypoxic and nutrient deficient state in the tumor, and alleviate the immunosuppressive effects of the tumor microenvironment. The loaded AIE photosensitizer can generate a large amount of ROS under light irradiation to induce immunogenic cell death and activate antigen-presenting cells, which can compensate for the lack of single gluta-

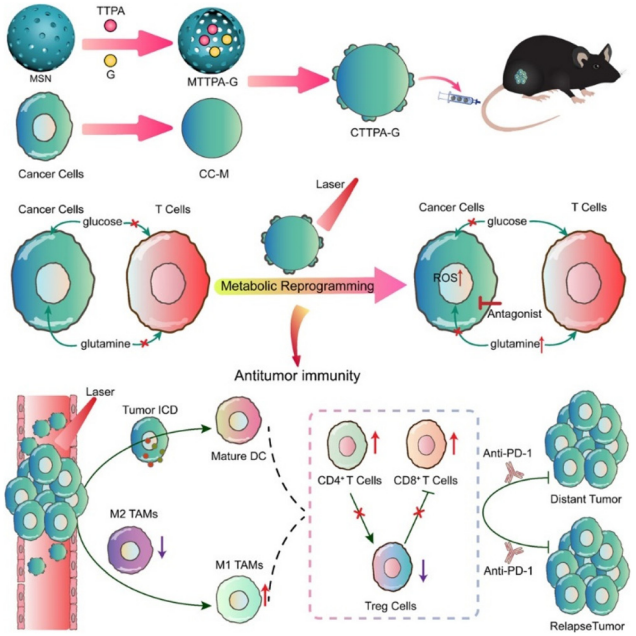

Fig. 4 Schematic diagram showing the preparation and process of biomimetic nanoplatform loading AIE photosensitizer and glutamine blockade for enhancing antitumor immunotherapy. Reproduced with permission from ref. 50. Copyright 2022 American Chemical Society.

mine antagonist therapy in antigen-presenting cells. After CTTPA-G treatment, the proliferation of primary tumors was effectively inhibited, and the tumor hypoxic state was significantly improved. Ultimately, CTTPA-G reduced nutrients for the cancer cells, induced immunogenic cell death, reshaped the tumor metabolism, and inhibited tumor proliferation.

On the other hand, red blood cell-mimicking nanoparticles can enhance targeting specificity, prolong circulation time, and reduce immunogenicity, which become a promising platform for drug delivery. Hong, Wang and coworkers reported the preparation strategy of red blood cell membrane-bound nanoparticles for tumoral photodynamic–immunotherapy.[37] The reported biomimetic nanoparticles were prepared through the self-assembly of the positively charged AIEgen (P2-PPh3) and the negatively charged polyinosinic:polycytidylic acid, followed by red blood cell membrane encapsulation. The consisted AIEgens play the role of photosensitizer for PDT, while polyinosinic:polycytidylic acid serves as an immune-stimulant to stimulate tumor and immune cells to activate immunity, which reduces tumor cell viability. The *in vivo* mice study depicted that the fabricated red blood cell-mimicking nanoparticles can accumulate in the tumor region and spleen, under the enhanced permeability and retention effect and homing effect of the red blood cell-mimicking shell, respectively. The light irradiation process can promote the ROS generation in tumor cells and induce the release of tumor antigens. The anti-tumor immunity is further enhanced by polyinosinic:polycytidylic acid in nanoparticles. Therefore, the reported strategy combines photodynamic properties and immunotherapy properties to achieve synergistic activation of the immune system for anti-tumor activity, which could be a future strategy for tumor treatment.

4 Conclusions and prospects

Biomimetic AIE nanoparticles have emerged as promising tools in the field of nanomedicine, particularly in disease diagnosis and phototherapy. By engineering AIE nanoparticles for phototherapy and incorporating biomimetic techniques, the field is witnessing advancements in achieving more precise and efficient image-guided phototherapy. The integration of cell membrane camouflaged nanoparticles offers several advantages, including enhanced targeting capabilities, prolonged circulation time, and evasion of the immune system. While cancer cell membranes and exosome membranes exhibit superior homologous cancer targeting capabilities, concerns remain regarding the presence of carcinogenic antigens, peptides, and proteins. On the other hand, blood cell membrane coating enables immune system evasion but lacks strong targeted site guidance. The use of a biomolecular core can improve the stability and biocompatibility of nanoparticles with AIEgen binding. However, no targeting ability is endowed by the biomolecular core. Peptide ligands can specifically navigate AIE nanoparticles to the targeted site, although the synthesis may require additional modifications of peptide and protection of peptide active region. Besides, ensuring biological functionality is the major concern of these biomimetic AIE nanoparticles, as they are susceptible to degradation by environmental conditions such as temperature, pH, and humidity. Among the biomimetic strategies, cell membrane encapsulation is the most complex, as the cell membrane must be freshly prepared through excretion and isolation from live cells, and the following coextrusion process of nanoparticles can be challenging in terms of nanoparticle size uniformity and cell membrane distribution. To address these challenges, a combination of biomimetic strategies can be employed. For instance, ligands can be attached to the surface of AIE nanoparticles to navigate them toward specific sites, while an additional blood cell coating on the outer layer can enhance their survival time. This dual approach offers a more comprehensive solution, optimizing both the targeted site approach and immune system response. Moreover, there is a wide range of biomaterials available for biomimetic applications, such as bacteria membranes, virus protein cages, and cellulose coating, which hold potential for various biomedical applications beyond AIE nanoparticles. Despite these challenges, the advancements in the field are inspiring the precise design of biomimetic AIE nanomaterials with optimized functions and structures, opening up possibilities for a diverse range of biomedical applications.

Author contributions

J. H. C. C., M. M. S. L., and E. Y. Y. proposed the topic of this review and drafted the manuscript. J. H. C. C., M. M. S. L.,

E. Y. Y., and R. T. K. K. discussed and organized the manuscript. J. H. C. C., M. M. S. L., E. Y. Y., R. T. K. K., J. W. Y. L., J. S., and B. Z. T. revised and proofread the manuscript.

Data availability

The authors confirm that no primary research results, software or code have been included and no new data were generated or analysed as part of this review.

Conflicts of interest

There are no conflicts to declare.

Acknowledgements

This work is supported by the Innovation and Technology Commission (ITC-CNERC14SC01), the Research Grants Council of Hong Kong (16303221 and HKUST PDFS2122-6S01) and Shenzhen Key Laboratory of Functional Aggregate Materials (ZDSYS20211021111400001).

References

1 G. Obaid, M. Broekgaarden, A. L. Bulin, H. C. Huang, J. Kuriakose, J. Liu and T. Hasan, *Nanoscale*, 2016, **8**, 12471–12503.
2 J. U. Menon, P. Jadeja, P. Tambe, K. Vu, B. Yuan and K. T. Nguyen, *Theranostics*, 2013, **3**, 152.
3 L. Chen, W. Hong, W. Ren, T. Xu, Z. Qian and Z. He, *Signal Transduction Targeted Ther.*, 2021, **6**, 225.
4 M. Zhang, Y. Du, S. Wang and B. Chen, *Drug Des., Dev. Ther.*, 2020, **14**, 5495–5503.
5 C. Y. Beh, R. P. Prajnamitra, L. L. Chen and P. C. H. Hsieh, *Molecules*, 2021, **26**, 5052.
6 B. Gidwani, V. Sahu, S. S. Shukla, R. Pandey, V. Joshi, V. K. Jain and A. Vyas, *J. Drug Delivery Sci. Technol.*, 2021, **61**, 102308.
7 E. Middha and B. Liu, *ACS Nano*, 2020, **14**, 9228–9242.
8 J. Mei, N. L. Leung, R. T. Kwok, J. W. Lam and B. Z. Tang, *Chem. Rev.*, 2015, **115**, 11718.
9 D. Ding, K. Li, B. Liu and B. Z. Tang, *Acc. Chem. Res.*, 2013, **46**, 2441.
10 Y. Li, Q. Wu, M. Kang, N. Song, D. Wang and B. Z. Tang, *Biomaterials*, 2020, **232**, 119749.
11 S. Liu, G. Feng, B. Z. Tang and B. Liu, *Chem. Sci.*, 2021, **12**, 6488–6506.
12 R. Zhang, Y. Duan and B. Liu, *Nanoscale*, 2019, **11**, 19241–19250.
13 X. Cai and B. Liu, *Angew. Chem., Int. Ed.*, 2020, **59**, 9868–9886.
14 N. Song, Z. Zhang, P. Liu, Y. W. Yang, L. Wang, D. Wang and B. Z. Tang, *Adv. Mater.*, 2020, **32**, 2004208.
15 Y. Shi, D. Zhu, D. Wang, B. Liu, X. Du, G. Wei and X. Zhou, *Coord. Chem. Rev.*, 2022, **471**, 214725.
16 M. Kang, Z. Zhang, N. Song, M. Li, P. Sun, X. Chen, D. Wang and B. Z. Tang, *Aggregate*, 2020, **1**, 80–106.
17 J. Dai, X. Wu, S. Ding, X. Lou, F. Xia, S. Wang and Y. Hong, *J. Med. Chem.*, 2020, **63**, 1996–2012.
18 Y. Dong, B. Liu and Y. Yuan, *J. Controlled Release*, 2018, **290**, 129–137.
19 M. Gao and B. Z. Tang, *Coord. Chem. Rev.*, 2020, **402**, 213076.
20 X. Liu, Y. Duan and B. Liu, *Aggregate*, 2021, **2**, 4–19.
21 V. Yazbeck, E. Alesi, J. Myers, M. H. Hackney, L. Cuttino and D. A. Gewirtz, *Adv. Cancer Res.*, 2022, **155**, 1–27.
22 J. Wang, N. Ninan, N. H. Nguyen, M. T. Nguyen, R. Sahu, T. T. Nguyen, A. Mierczynska-Vasilev, K. Vasilev, V. K. Truong and Y. Tang, *ACS Appl. Mater. Interfaces*, 2024, **16**, 18449–18458.
23 Y. Li, D. Zhang, Y. Yu, L. Zhang, L. Li, L. Shi, G. Feng and B. Z. Tang, *ACS Nano*, 2023, **17**, 16993–17003.
24 K. Ding, L. Wang, J. Zhu, D. He, Y. Huang, W. Zhang, Z. Wang, A. Qin, J. Hou and B. Z. Tang, *ACS Nano*, 2022, **16**, 7535–7546.
25 T. Gao, Y. Wu, W. Wang, C. Deng, Y. Chen, L. Yi, Y. Song, W. Li, L. Xu, Y. Xie, L. Fang, Q. Jin, L. Zhang, B. Z. Tang and M. Xie, *ACS Nano*, 2021, **15**, 11908–11928.
26 A. Song, Y. Wang, J. Xu, X. Wang, Y. Wu, H. Wang, C. Yao, H. Dai, Y. Zhang, Q. Wang and C. Wang, *Nano Today*, 2024, **54**, 102109.
27 N. M. Molino and S. W. Wang, *Curr. Opin. Biotechnol.*, 2014, **28**, 75–82.
28 E. J. Lee, N. K. Lee and I. S. Kim, *Adv. Drug Delivery Rev.*, 2016, **106**, 157–171.
29 H. Iqbal, T. Yang, T. Li, M. Zhang, H. Ke, D. Ding, Y. Deng and H. Chen, *J. Controlled Release*, 2021, **329**, 997–1022.
30 J. Herre, S. Gordon and G. D. Brown, *Mol. Immunol.*, 2004, **40**, 869–876.
31 G. D. Brown, J. Herre, D. L. Williams, J. A. Willment, A. S. Marshall and S. Gordon, *J. Exp. Med.*, 2003, **197**, 1119–1124.
32 Y. Wu, Q. Jin, Y. Chen, H. Li, C. Deng, Z. Sun, Y. Li, B. Wang, H. Li and C. Wu, *Biomater. Sci.*, 2020, **8**, 5282–5292.
33 J. Zhang, X. He and B. Z. Tang, *ACS Nano*, 2024, **18**, 3199–3213.
34 L. Martínez-Jothar, S. Doulkeridou, R. M. Schiffelers, J. Sastre Torano, S. Oliveira, C. F. van Nostrum and W. E. Hennink, *J. Controlled Release*, 2018, **282**, 101–109.
35 Z. Sun, X. Hua, M. Bao, W. Xu, M. Kang, H. Mo, G. Hu, G. Yue, X. Chen, S. Mo, Z. Zhang, D. Wang and J. Song, *Nano Today*, 2024, **54**, 102107.
36 P. Xie, H. Ling, M. Pang, L. He, Z. Zhuang, G. Zhang, Z. Chen, C. Weng, S. Cheng, J. Jiao, Z. Zhao, B. Z. Tang and L. Rong, *Adv. Ther.*, 2022, **5**, 2200076.

37 J. Dai, M. Wu, Q. Wang, S. Ding, X. Dong, L. Xue, Q. Zhu, J. Zhou, F. Xia, S. Wang and Y. Hong, *Natl. Sci. Rev.*, 2021, **8**, nwab039.
38 X. Xu, G. Deng, Z. Sun, Y. Luo, J. Liu, X. Yu, Y. Zhao, P. Gong, G. Liu, P. Zhang, F. Pan, L. Cai and B. Z. Tang, *Adv. Mater.*, 2021, **33**, e2102322.
39 Y. Duo, M. Suo, D. Zhu, Z. Li, Z. Zheng and B. Z. Tang, *ACS Appl. Mater. Interfaces*, 2022, **14**, 26394–26403.
40 J. Dai, Z. Chen, S. Wang, F. Xia and X. Lou, *Mater. Today Bio*, 2022, **15**, 100279.
41 Z. Sun, J. Liu, Y. Li, X. Lin, Y. Chu, W. Wang, S. Huang, W. Li, J. Peng, C. Liu, L. Cai, W. Deng, C. Sun and G. Deng, *Adv. Mater.*, 2023, **35**, e2208555.
42 X. Yang, T. Yang, Q. Liu, X. Zhang, X. Yu, R. T. K. Kwok, L. Hai, P. Zhang, B. Z. Tang, L. Cai and P. Gong, *Adv. Funct. Mater.*, 2022, **32**, 2206346.
43 B. Li, W. Wang, L. Zhao, M. Li, D. Yan, X. Li, J. Zhang, Q. Gao, Y. Feng, J. Zheng, B. Shu, Y. Yan, J. Wang, H. Wang, L. He, Y. Wu, S. Zhou, X. Qin, W. Chen, K. Qiu, C. Shen, D. Wang, B. Z. Tang and Y. Liao, *Adv. Mater.*, 2024, **36**, e2305378.
44 W. Wang, Y. Gao, M. Zhang, Y. Li and B. Z. Tang, *ACS Nano*, 2023, **17**, 7394–7405.
45 S. Ning, T. Zhang, M. Lyu, J. W. Y. Lam, D. Zhu, Q. Huang and B. Z. Tang, *Biomaterials*, 2023, **295**, 122034.
46 S. Ning, M. Lyu, D. Zhu, J. W. Y. Lam, Q. Huang, T. Zhang and B. Z. Tang, *ACS Nano*, 2023, **17**, 10206–10217.
47 J. Dai, M. Wu, Y. Xu, H. Yao, X. Lou, Y. Hong, J. Zhou, F. Xia and S. Wang, *Bioeng. Transl. Med.*, 2023, **8**, e10417.
48 B. Li, W. Wang, L. Zhao, Y. Wu, X. Li, D. Yan, Q. Gao, Y. Yan, J. Zhang, Y. Feng, J. Zheng, B. Shu, J. Wang, H. Wang, L. He, Y. Zhang, M. Pan, D. Wang, B. Z. Tang and Y. Liao, *Nat. Nanotechnol.*, 2024, 1–12.
49 Y. Li, R. Zhang, Q. Wan, R. Hu, Y. Ma, Z. Wang, J. Hou, W. Zhang and B. Z. Tang, *Adv. Sci.*, 2021, **8**, 2102561.
50 W. Xie, B. Chen, H. Wen, P. Xiao, L. Wang, W. Liu, D. Wang and B. Z. Tang, *ACS Nano*, 2022, **16**, 10742–10753.
51 J. Su, Z. Yao, Z. Chen, S. Zhou, Z. Wang, H. Xia, S. Liu and Y. Wu, *Small*, 2022, **18**, e2203448.
52 J. Cui, F. Zhang, D. Yan, T. Han, L. Wang, D. Wang and B. Z. Tang, *Adv. Mater.*, 2023, **35**, e2302639.
53 L. Zhang, Z. Wang, R. Zhang, H. Yang, W. J. Wang, Y. Zhao, W. He, Z. Qiu, D. Wang, Y. Xiong, Z. Zhao and B. Z. Tang, *ACS Nano*, 2023, **17**, 25205–25221.
54 S. Ning, M. Suo, Q. Huang, S. Gao, K. Qiao, M. Lyu, Q. Huang, T. Zhang and B. Z. Tang, *Nano Today*, 2024, **54**, 102106.
55 H. Shen, Y. Li, X. Kang, J. Wu, R. Chen, X. Wei, X. Zhang, J. Qi and Q. Liu, *ACS Appl. Nano Mater.*, 2023, **6**, 6056–6065.
56 Y. Li, X. Fan, Y. Li, L. Zhu, R. Chen, Y. Zhang, H. Ni, Q. Xia, Z. Feng, B. Z. Tang, J. Qian and H. Lin, *Nano Today*, 2021, **41**, 101333.
57 H. Cao, H. Gao, L. Wang, Y. Cheng, X. Wu, X. Shen, H. Wang, Z. Wang, P. Zhan, J. Liu, Z. Li, D. Kong, Y. Shi, D. Ding and Y. Wang, *ACS Nano*, 2022, **16**, 13992–14006.
58 Y. Lin, M. Yi, X. Guan, E. Chen, L. Yang, S. Li, Y. Li and L. Zhang, *J. Nanobiotechnol.*, 2023, **21**, 49.
59 P. Cheng, X. Du, S. Chen, K. Chen, Y. Yuan, J. Shao, Q. Shen, P. Sun and Q. Fan, *ACS Appl. Nano Mater.*, 2023, **6**, 10736–10745.
60 M. Suo, H. Shen, M. Lyu, Y. Jiang, X. Liao, W. Tang, Y. Pan, T. Zhang, S. Ning and B. Z. Tang, *Small*, 2024, **17**, e2400666.
61 S. Ning, X. Zhang, M. Suo, M. Lyu, Y. Pan, Y. Jiang, H. Yang, J. W. Y. Lam, T. Zhang, L. Pan and B. Z. Tang, *Cell Rep. Phys. Sci.*, 2023, **4**, 101505.
62 H. H. Gustafson, D. Holt-Casper, D. W. Grainger and H. Ghandehari, *Nano Today*, 2015, **10**, 487–510.
63 J. A. Mills, F. Liu, T. R. Jarrett, N. L. Fletcher and K. J. Thurecht, *Biomater. Sci.*, 2022, **10**, 3029–3053.
64 R. Kalluri and V. S. LeBleu, *Science*, 2020, **367**, eaau6977.
65 S. Kamerkar, V. S. LeBleu, H. Sugimoto, S. Yang, C. F. Ruivo, S. A. Melo, J. J. Lee and R. Kalluri, *Nature*, 2017, **546**, 498–503.
66 C. Gong, J. Tian, Z. Wang, Y. Gao, X. Wu, X. Ding, L. Qiang, G. Li, Z. Han, Y. Yuan and S. Gao, *J. Nanobiotechnol.*, 2019, **17**, 1–18.
67 B. Li, W. Wang, L. Zhao, D. Yan, X. Li, Q. Gao, J. Zheng, S. Zhou, S. Lai, Y. Feng, J. Zhang, H. Jiang, C. Long, W. Gan, X. Chen, D. Wang, B. Z. Tang and Y. Liao, *ACS Nano*, 2023, **17**, 4601–4618.